ALMA MEMO No. 363

VELOCITY OF THE EFFECTIVE TURBULENCE LAYER AT CHAJNANTOR ESTIMATED FROM 183 GHZ MEASUREMENTS

Guillermo Delgado
Onsala Space Observatory / European Southern Observatory
Casilla 19001, Santiago 19, Chile
Email: gdelgado@eso.org

Lars-Åke Nyman
Onsala Space Observatory / European Southern Observatory
Casilla 19001, Santiago 19, Chile
Email: lnyman@eso.org

Abstract – The cross-correlation of the precipitable water vapour (PWV) variation of two water vapour radiometers placed at the ends of a 300-m baseline along the E-W direction was used to measure the time lag between the structures seen at each radiometer. With a fixed separation between the two radiometers, and observing with parallel beams, we can determine the effective speed of the turbulence layer.

A linear relation between the turbulence layer speed and the ground wind speed was found indicating that the turbulence speed is roughly twice as high as the ground measured wind speed.

The temporal phase structure function was calculated, showing that the turbulence screen goes through a daily cycle associated with the insolation, with a well-defined layer structure at the extremes of the cycle.

The cross-correlation method allows the reliable measurement of the effective turbulence speed for about 90% of the day, apparently associated with the wind direction and the time when the turbulence layer is high up (the definition of "high up" is still uncertain). This implies that with a variation of this method, by moving the beams in the sky, we can continuously measure the height of the turbulence layer during most of the day, providing a very useful tool to assess the dynamics of the turbulence layer.

Introduction

One of the main concerns for ALMA is the imaging quality possible to achieve. The presence of water vapour in the atmosphere degrades the phase characteristics of a plane wave travelling through the troposphere. The reason for this is the higher refractive index of the water vapour and the poor mixing of water vapour with the "dry air" components (other gaseous components of the air at the tropospheric heights).

A proposed technique to correct for the phase variation introduced by the water vapour in the atmosphere is the measurement of the brightness temperature along the line of sight and then relate this brightness temperature fluctuations to phase fluctuations. This is possible due to the low dispersion of millimetre and sub-millimetre wavelengths in the troposphere and through the use of linear relations between electric path length delay and the PWV content [1].

At Chajnantor, the selected site for ALMA, we have started a series of experiments to assess the possibility of using this phase correction technique [2, 3]. Our first results indicate that phase correction is possible with good results (up to 75% phase correction), but the phase correction possible to achieve presents variations during the day [4]. A correlation between the success of the phase correction and the height of the turbulence layer has been proposed, with better phase correction results when the height of the turbulence layer is high. As discussed in [4], this can be an effect of the setup because of the large far-field distance of the interferometer.

In order to confirm this result we need a reliable method to continuously estimate the height of the turbulence layer at Chajnantor. Presently there are two methods in use at Chajnantor: the first one are the tropospheric profiles obtained from radiosonde launches at Chajnantor and the second method uses the two-interferometer technique [5]. While the first method is the most reliable because it directly indicates the presence and real altitude of water vapour layers in the atmosphere over the site, it is cumbersome and we do not have good coverage over the year or even during the day mainly because of the logistic difficulties of organising radiosonde launch campaigns. The two-interferometer method, can in principle be used at all times, but faces other practical problems. The most severe limitation is the one imposed by the need to have simultaneously working the two interferometers and a weather station measuring wind speed and direction at Chajnantor. This sounds in principle trivial, but the reality has proven to be different [5]. Besides, there is the also the problem of estimating the wind aloft from ground measurements.

We propose here another method to find the height of the turbulence layer. This method relies on the recently added capability of the 183 GHz water vapour radiometers (WVR) to move the primary mirror, making it possible to orient the beam to almost any position on the sky. The idea of this method is based on the assumption of a frozen screen approximation of the turbulence layer. If the PWV signal from one WVR is cross-correlated with the PWV signal from the other WVR, with both beams parallel, we should be able to see the passing turbulent structures from one beam to the other in a time corresponding to the transit time over the baseline. With a known transit time, we can obtain directly the effective turbulence speed. Now, if we move the primary mirror of both WVR in order to geometrically cross the two beams at different heights along the baseline between the WVR, we can find a position where the time lag of the cross-correlation is zero. This should correspond to the height of the turbulence layer. Variations of this method based on the fixed geometry can be used to optimise the determination of the turbulence height with fewer measurements.

A first approach to assess the feasibility of this method is done here by calculating the lag time given by the cross-correlation between the two WVR while they are oriented towards an elevation of 37.75° (in the direction of satellite Intelsat IS 605). As long as the WVR beams are kept parallel, independent of the relative orientation in the sky, the projected baseline will remain constant and hence a direct determination of the speed of the turbulent screen will be possible.

Cross-correlation results

The cross-correlation of the time series of the WVR is done by reading a data block of the West WVR time series, defining a base frame with a constant length. This data block is compared (cross-correlated) with a moving window of the East WVR time series. The cross-correlation is defined by:

$$r(\tau) = \frac{\sum_i T_W(t_i) T_E(t_i + \tau)}{\sqrt{\sum_i (T_W(t_i))^2} \sqrt{\sum_i (T_E(t_i + \tau))^2}} \qquad (1)$$

with i defining the length of the comparison windows, and τ varying symmetrically around the centre time of the fixed base frame on the West WVR.

The attained maximum of the cross-correlation peaks at a certain τ value that corresponds to the time lag of the PWV signal between the two WVR. This time lag, over the fixed baseline length, defines the effective speed of the turbulence. The difference between the size of the data block frame and the comparison window defines twice the time lag possible to measure.

To define the length of the data block frame and the comparison window we can observe the PWV series. In the centre plot of Figure 1 we see the complete PWV variation during day 15/11/99 and in the smaller plots around it there are one-hour details of this PWV variation for the two WVR. From the one-hour detail showing 3 to 4 hours UT time (lower plot to the left) the structures seen are about 900 seconds in width, with an average turbulence layer wind speed of ~10 m/s at this time, these structures have a minimum size of ~9000 m. On the 16 to 17 hours UT plot (upper plot to the left), the structures have a width of about 200 seconds, with an average turbulence wind speed of 16 m/s at this time, the structures present a minimum width of ~3000 m. Since the turbulent structures vary in size during the day, then the optimal size of the data block frame is given by the wind speed at the time of the measurement, during periods of lower wind speed we need a 3-times longer data block frame to capture the structures as compared with those times with higher wind speed.

Figure 2 shows the maximum of the cross-correlation for the data block frames dividing the complete day 15/11/99. The maximum cross-correlation coefficient is the peak cross-correlation value within the time lag allowed by the measurement. The two cases presented correspond to a data block frame of 300 sec (5 minutes) and 900 sec (15 minutes) with a comparison window of 180 sec (3 minutes) and 540 sec (9 minutes) respectively. It can be seen that both time frames (with associated windows) give about the same result. With a data block frame of 300 sec and a comparison window of 180 sec, we can measure a ±60 sec lag time, which determines that turbulence speeds lower than ±5 m/s can not be detected. With a data block frame of 900 sec and a comparison window of 540 sec, we can measure a ±180 sec lag time, defining a minimum turbulence speed detection of ±1.7 m/s.

Examples of the cross-correlation for day 15/11/99 over the 5-minute frames are given in Figure 3, where the results are given in one-hour intervals, with twelve measurements in each one. The label indicates the starting UT hour represented in each plot, coinciding with those times indicated in Figure 1. The heavy curve in black dots represents the hourly average of the twelve 5-minute frames. The two lower plots corresponding to 16 UT and 22 UT show well defined cross-correlation peaking in a clear time lag within the measured window. The plot corresponding to 3 UT also show a clear peak of the time lag, but some of them are already on the border or out of the edge of the measured window, the measuring of the time lag will clearly benefit from a larger window. In the case of 9 UT we can see that the lack of a correlation is because the signals are not correlated at all, increasing the measured window does not help here.

On the 300 sec frame, we have 288 average cross-correlation coefficients calculated during the 24-hour recording, discarding those ones with maximum amplitude lower than 0.6, we obtain 156 points with valid data (54% valid data). Considering the longer frame of 900 sec, we have 81 data points with correlation coefficient over 0.6 out of a total of 94 measured over the 24-hour period (86% valid data).

The valid cross-correlation coefficients provide a time lag and this value in turn, over the fixed baseline length, gives an “effective turbulence speed” along the baseline. This turbulence layer speed is the signature of the dominant structures in the turbulence layer and might be different from the actual wind speed at that height, but it is the one creating the phase variations seen from ground.

This value of effective turbulence speed can be compared with the ground wind speed projected along the baseline. Figure 4 shows the comparison between these two speeds after removal of the scattered data points (larger than ±50 m/s for the effective turbulence speed). A linear fit indicates that the proportionality factor between the effective turbulence speed along the baseline and the projected ground wind is given by 1.8 for the 300 sec frame and 1.6 for the 900 sec frame. Since the wind aloft should depend on the height, this linear relation between the projected ground wind speed and the measured turbulence layer speed might be indicating that in Chajnantor there is a linear relation between the actual ground wind speed and the height of the turbulence layer.

The origin of the negative speeds, both in the effective turbulence speed and the projected ground wind speed, are in an inversion of the predominant ground wind speed. As can be seen in Figure 5, this inversion is produced at around 8 UT (4:00 local time) and lasts for a few hours. This change of direction coincides

with the absolute minimum ground wind speed as can be seen in Figure 6, were we have plotted the cosine of the ground wind direction, referred to the E-W baseline, against the absolute value of the ground wind speed. A value of 1 indicates a wind coming from the West, while a value of –1 indicates a wind coming from the East. An intermediate value of zero indicates a wind perpendicular to the baseline, coming from the North (most likely) or the South (rare).

In Figure 7 we have the comparison between all the maximum cross-correlation values for day 15/11/99, using a 900 sec frame, with the projected ground wind speed (upper plot) and the wind direction (lower plot). For the wind direction we used again the cosine of the wind direction referred to the E-W baseline. The cross-correlation does not seem to be related to the ground wind speed, even when lower values of cross-correlation and a higher scatter can be seen at low wind speeds. On the other hand, there seems to be a clear relation between the cross-correlation and the wind direction, with a decrease in the cross-correlation when the wind blows through the North to start blowing from the East (period of wind direction inversion). This is reasonable since during this time we have the coincidence of the minimum ground wind speeds and the wind blowing perpendicular to the baseline.

From radiosonde measurements it is possible to estimate the height of the turbulence layer by observing the anomalies on the vertical temperature distribution, these measurements indicate the height at which an inversion layer is present and we assume that the water vapour is trapped there creating a turbulence layer. For days 6 and 7 November 1999, were we have radiosonde launches, we compare the result of the cross-correlation analysis with the height of the turbulence layer estimated from the radiosonde profiles. Figure 8 indicates that there is a tendency to have a lower cross-correlation when the turbulence height is low. This in turn seems to occur during the first half of the UT day, or equivalently the local night-time between 20:00 to 8:00 local time, this again yields to some sort of relation between the height of the turbulence layer and the ground wind speed.

Temporal phase structure function

The atmospheric phase variations due to water vapour can be characterised by the square root of the spatial phase structure function, defined as the root mean square of the phase variations over a given baseline length. Thanks to the frozen screen approximation, we can relate the spatial phase fluctuation to the temporal phase fluctuation and thus, from the phase time series, it is possible to derive the temporal phase structure function. According to this, we obtain a function of the form [6]:

$$D_\phi(t) = \left\langle \left(\phi(t_0) - \phi(t_0 + t)\right)^2 \right\rangle = K t^\alpha \qquad (2)$$

where α is a exponent with its value depending in the turbulence layer characteristics. For a thick (3D) layer the exponent is 0.83, for a thin (2D) layer, the exponent is 0.33. Intermediate values of α can be explained by a superposition of thick and thin layers [6] or a transition between different layer thickness.

When the temporal phase structure function is evaluated for *t*, it is found that there are two very distinct zones. The first one, for small values of *t*, increases following the power law function with the exponent α and a second zone, at large values of *t*, where the function saturates to a value σ_ϕ that represents the rms phase over the 300-m baseline (see Figure 9).

From the PWV time series it is possible to derive the phase variation time series by converting the PWV variations to path delay variations and from these values to phase variations through a linear relation as described elsewhere [3].

We computed the temporal phase structure functions of the phase time series of the WVR for the day 15/11/99, dividing the day in 10-minute blocks. No instrumental error was removed from the time series, even when at times of very low atmospheric activity there is evidence for the presence of noise at around 10 UT (Figure 9 a)), as compared with times with higher phase noise at around 18 UT (Figure 9 b)).

The daily variation of the α exponent for the observed day 15/11/99 is shown in Figure 10. It can be seen that most of the day, between 0 UT and ~12 UT (20:00 and 8:00 local time) the turbulence layer shows thin characteristics. While for a shorter time between 15 UT and 20 UT (13:00 and 16:00 local time), the turbulence layer is definitively thick. At sunrise (~12 UT), there is a sharper change between the two types of turbulence layer than during the afternoon (between 16:00 and 20:00 local time) when the atmosphere changes state more slowly over a four hour period.

The square root of the average value of the temporal phase structure function after reaching saturation, at long time values, gives directly the rms phase for the observed period. The variation of the rms phase during the day is very much correlated with the daily variation of the α exponent (Figure 10).

A comparison with the ground wind speed and direction (seen in Figure 5), shows that the α exponent is not related to the wind direction, but might be related to the wind speed (or rather, probably the wind speed, the rms phase, and the α exponent are all related to the insolation, defining most of the daily tropospheric cycles observed at Chajnantor).

From the temporal phase structure function data obtained every ten minutes it is also possible to obtain the "corner time," this is the time when the temporal phase structure function saturates to reach an approximately flat value (the α exponent becomes zero). This average value at larger times corresponds to the rms phase for the sampled period. The intersection of the exponential function with the α coefficient for low times and the rms phase at larger time values define a time known as "corner time". This corner time t_c can be related to the wind aloft v by [6]:

$$v = s(\alpha)\frac{B}{t_c}$$

where B is the baseline length. And $s(\alpha)$ is a scaling function obtained from numerical simulations [6]:

$$s(\alpha) = 0.91\alpha + 0.35 \pm 0.03$$

While this corner value gives the velocity aloft, this value does not have an indication of the wind direction and thus we did not attempt to correlate it with the turbulence velocity determined with the cross-correlation method. Figure 11 shows the result of the velocity aloft calculation and the projected ground speed. Here we can see that the two velocities correspond to each other very closely, without showing the relation found through the cross-correlation that indicated that the wind aloft was about twice the projected ground wind speed. This is probably due to the size of the data block used, since from Figure 9 we can see that the saturated area is just beginning. Since this is not relevant for uor work we will not go in more details here.

Conclusions and discussion

We have successfully used the cross-correlation of the PWV signal from the two WVR to measure the speed of the turbulence layer along the 300-m E-W baseline of the WVRs. Comparing this effective turbulence speed with the projected ground wind speed, we obtain a linear fit indicating that the turbulence speed is roughly twice as high as the ground wind projected on the baseline. From radiosonde data [7] we have that the wind speed is twice as high as the ground speed at variable heights between 500 to 1,000 m. Adding the value of the actual height of the turbulence layer, at the same time as the speed is determined, we might be able to find a more accurate relation between the ground wind speed and the turbulence layer speed.

The relation obtained between ground wind speed and the speed of the turbulence layer might introduce a revision of the quantitative results at [5] that indicate that 70% of the time the turbulence layer is below 500 m. Using a speed for the turbulence layer twice as high as the ground speed, the updated result is that 70% of the time the turbulence layer is below 1,000 m. This is still a very good case for the matching of the

astronomical and WVR beams on the final telescope design. According to Gibb and Harris [8], with the actual design parameters of ALMA and with the turbulence layer at 1,000 m, the overlap between the astronomical and WVR beams is better than 80% at 2 airmasses.

The relation between the effective turbulence speed and the ground wind speed is affected by the fact that our results are considering about 90% of the data. These data seem to be concentrated during those times when the turbulence layer is high and thick and the wind speed is high and blowing mostly parallel to the baseline, according to wind and radiosonde measurements and the temporal phase structure results.

We also found that the correlation is difficult to achieve or fails completely when the turbulence layer is too close to the ground. This coincides with the local night-time when the PWV and the phase variations are at a minimum. At this time of the day the wind speed is at a minimum and goes through an inversion of the predominant West direction blowing at times perpendicular to the baseline. We have to remind also that our method has a minimum speed detection of ±1.7 m/s. To conclude, we think that the loss of correlation under these conditions is because the very low and thin turbulent layer is not well measured too close to the ground.

During the local night time, not only the turbulence layer is low, but also the ground wind reaches a minimum value, goes through an inversion in a complete 360 degrees direction change over a period of ~4 hours and then starts to increase speed at 12 UT or 8:00 local time. This can also explain the result in [5] that found a poor correlation between the two-interferometers when the wind speed is low. In this case the bad correlation is due to the low turbulence layer during night-time.

The results indicate that we can use the cross-correlation method to follow the dynamics of the turbulence layer during most of the day, and we will be able to determine the minimum detectable height of the turbulence layer. These results will be of high relevance for the characterisation of the turbulence layer.

Acknowledgements

The authors acknowledge the many fruitful discussions with Yasmin Robson (MRAO). Angel Otárola (ESO) is vital in keeping the instruments running through all the altiplanic storms.

Important part of the funding for this project came out of the budget of Onsala Space Observatory provided by the Swedish Natural Science Council (NFR).

References

[1] A. Thompson, J. Moran, and G. Swenson, *Interferometry and Systhesis in Radio Astronomy*, Krieger Publishing Company, 1994.

[2] G. Delgado, A. Otárola, V. Belitsky, D. Urbain, and P. Martin-Cocher, "The Determination of Precipitable Water Vapour at Llano de Chajnantor from Observations of the 183 GHz Water Vapour Line," ALMA Memo Series No. 271, 1999.

[3] G. Delgado, A. Otárola, L-Å. Nyman, R. Booth, V. Belitsky, D. Urbain, R. Hills, Y. Robson, and P. Martin-Cocher, "Phase Correction of Interferometer Data at Mauna Kea and Chajnantor," ALMA Memo Series No. 332, 2000.

[4] G. Delgado, L-Å. Nyman,, A. Otárola, , R. Hills, and Y. Robson "Phase Cross-correlation of a 11.2 GHz Interferometer and 183 GHz Water Line Radiometers at Chajnantor," ALMA Memo Series No. 361, 2001.

[5] Y. Robson, R. Hills, J. Richer, G. Delgado, L-Å. Nyman, A. Otárola, and S. Radford, “Phase Fluctuations at the ALMA Site and the Height of the Turbulent Layer,” to be published in the Proceedings of the IAU-2000 Conference, Marrakech, 2000.

[6] M. Holdaway, S. Radford, F. Owen, and S. Foster, “Data Processing for Site Testing Interferometers,” ALMA Memo Series No. 129, 1995.

[7] http://alma.sc.eso.org/

[8] A. Gibbs and A. Harris, “The Overlap of the Astronomical and WVR Beams,” ALMA Memo Series No. 330, 2000.

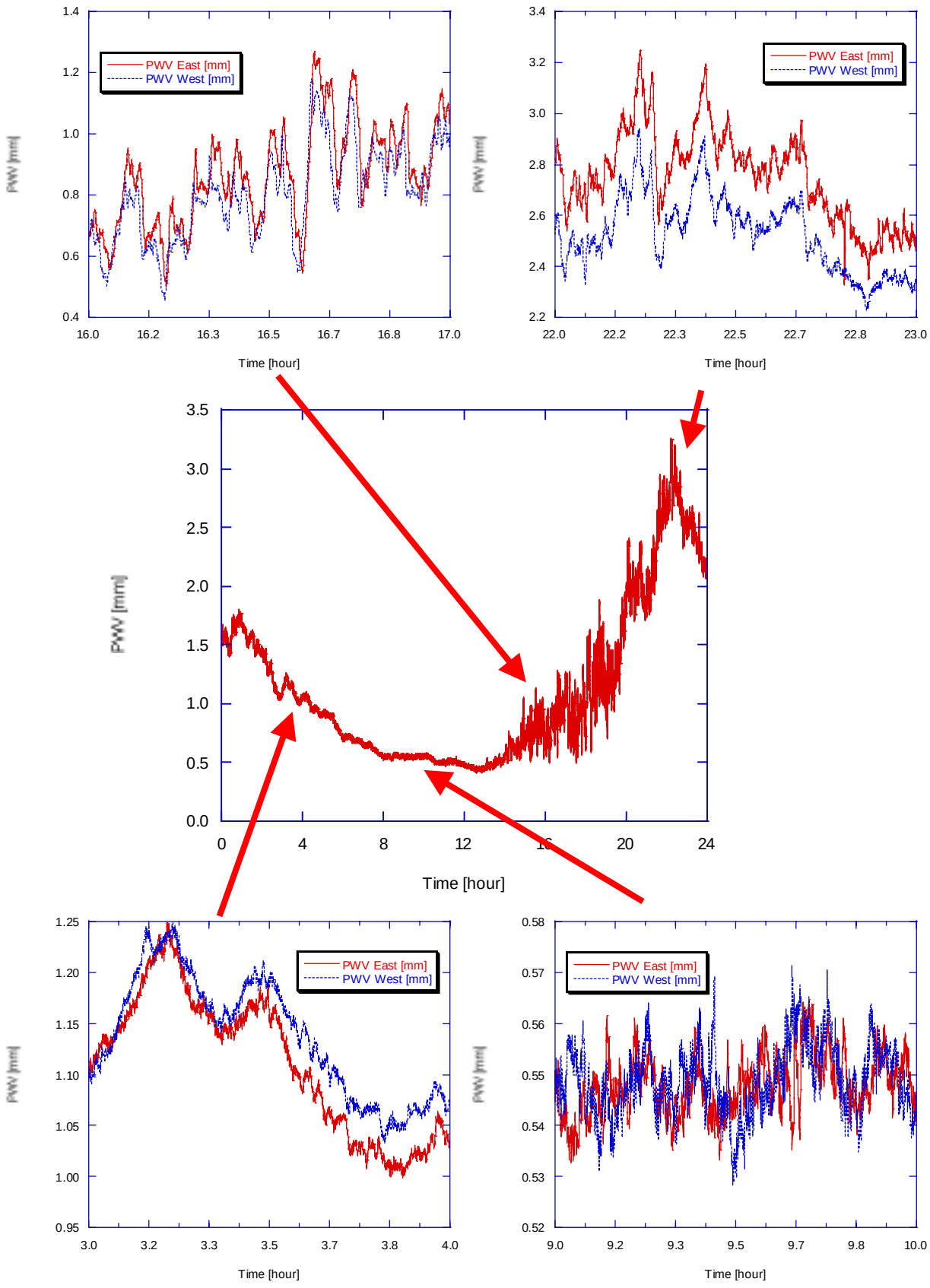

Fig. 1 Time series of the PWV for day 15/11/99 (centre plot). The smaller plots represent one-hour details for representative periods of the day.

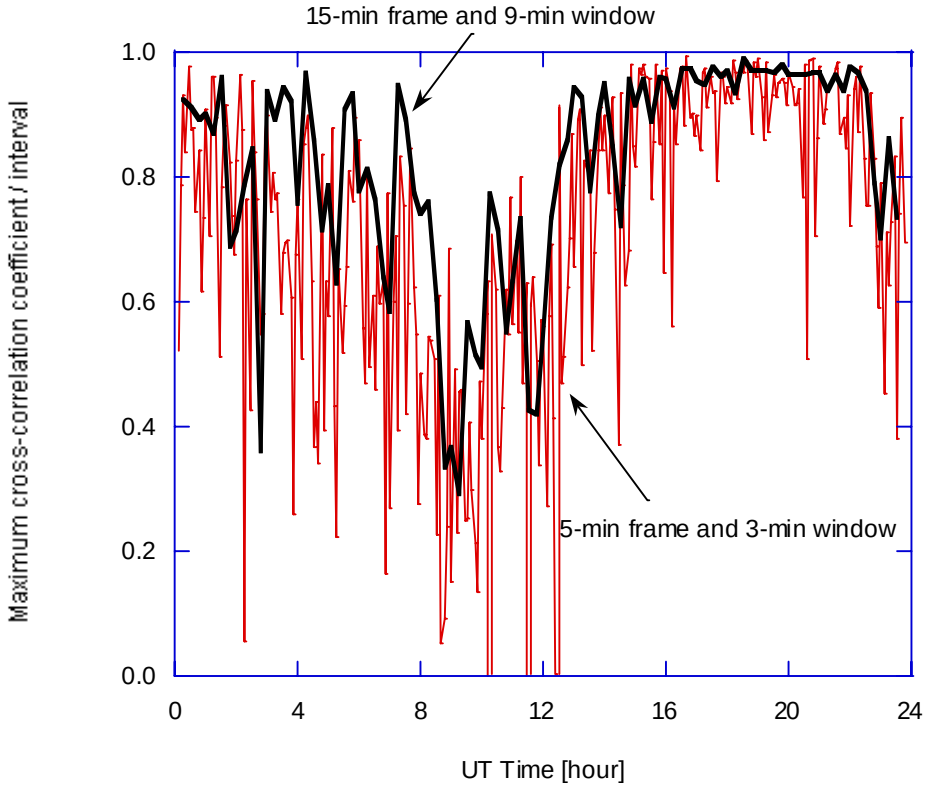

Fig. 2 Maximum of the cross-correlation for the data block frames dividing the complete day 15/11/99, showing the data corresponding to a data block frame of 300 sec (5 minutes) with a comparison window of 180 sec (3 minutes) (thin line) and a data block frame of 900 sec (15 minutes) and a comparison window of 540 sec (9 minutes) (thick line).

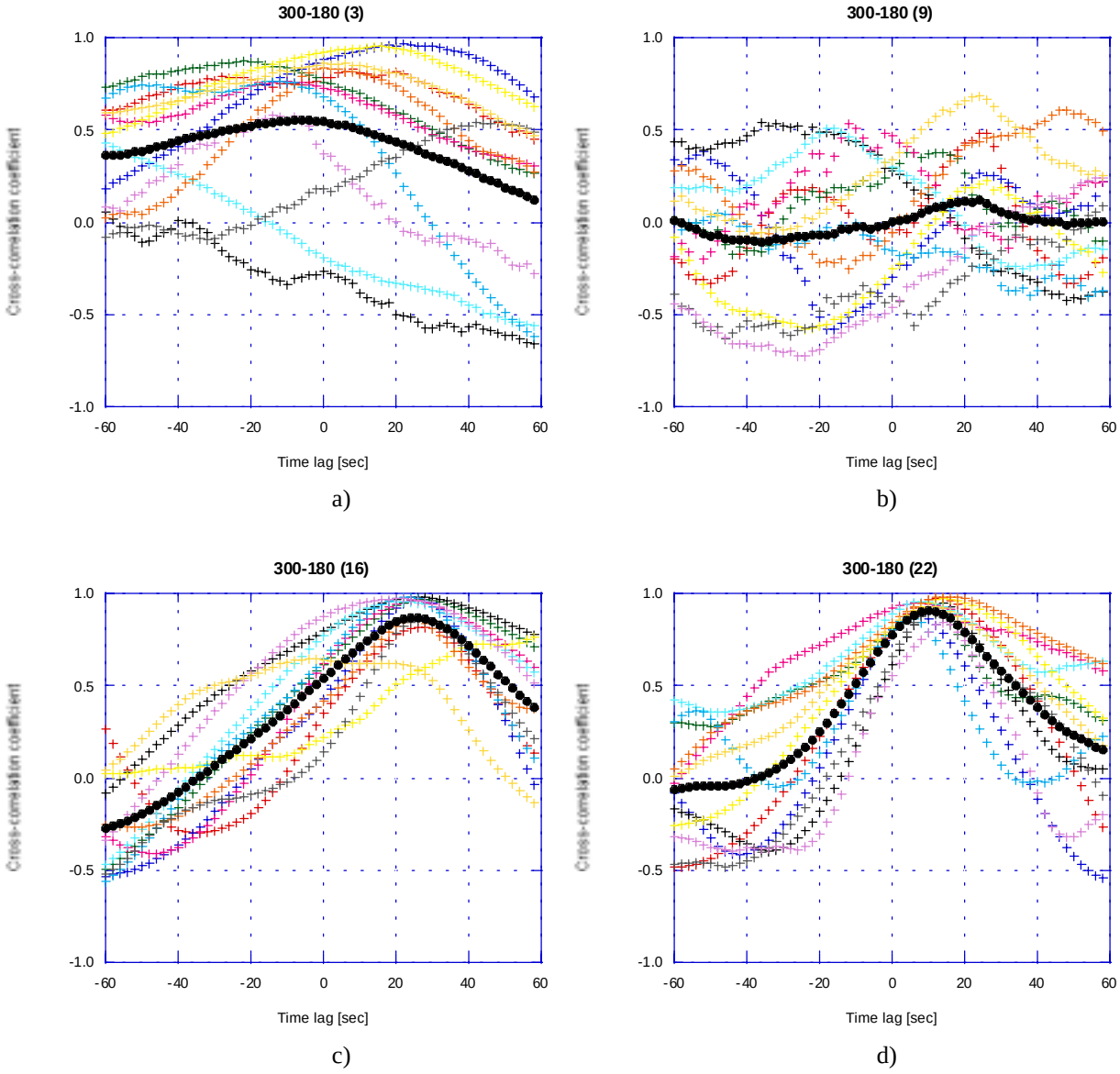

Fig. 3 Examples of some hourly result of the cross-correlation between the PWV signal of the two WVR at the ends of a 300-m baseline for day 15/11/99. In each plot the black dots represent the average of the twelve 5-minute measurements during the one-hour interval. The plots correspond to different UT times with a) at 3 UT (23:00 local time), b) 9 UT (05:00 local time), c) 16 UT (12:00 local time), and d) 22 UT (18:00 local time)

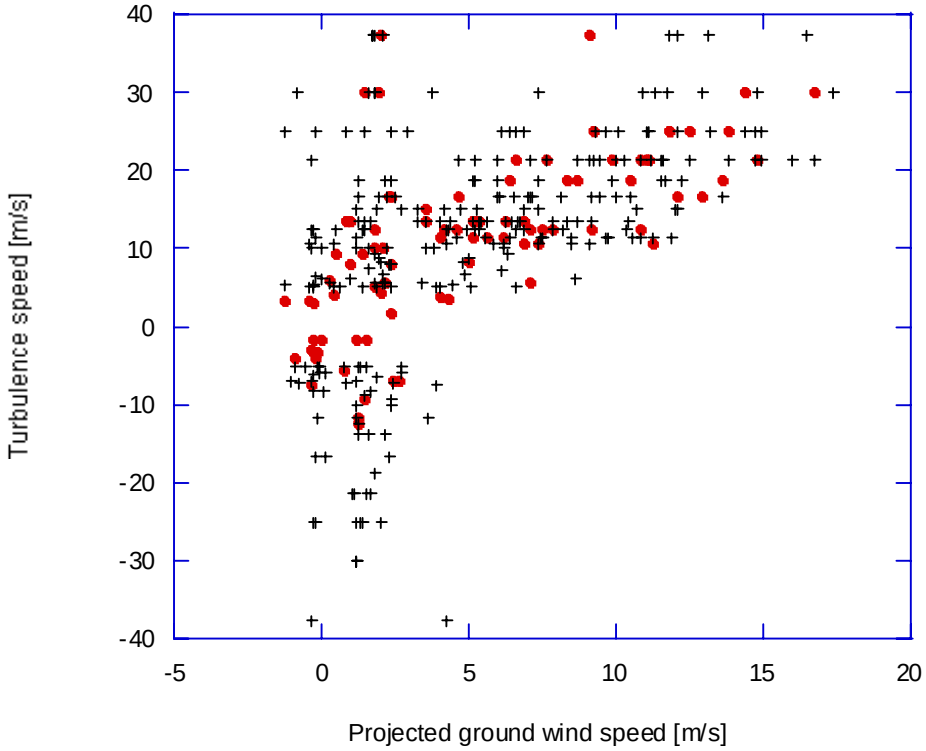

Fig. 4 Scatter plot of all the measured wind speed data points versus the projected ground wind speed along the E-W baseline for day 15/11/99. The data was clipped to eliminate the points indicating a turbulence speed greater than ±50 m/s. The filled dots represent the data measured with a 900 sec frame and the crosses indicate those points measured using a 300 sec frame.

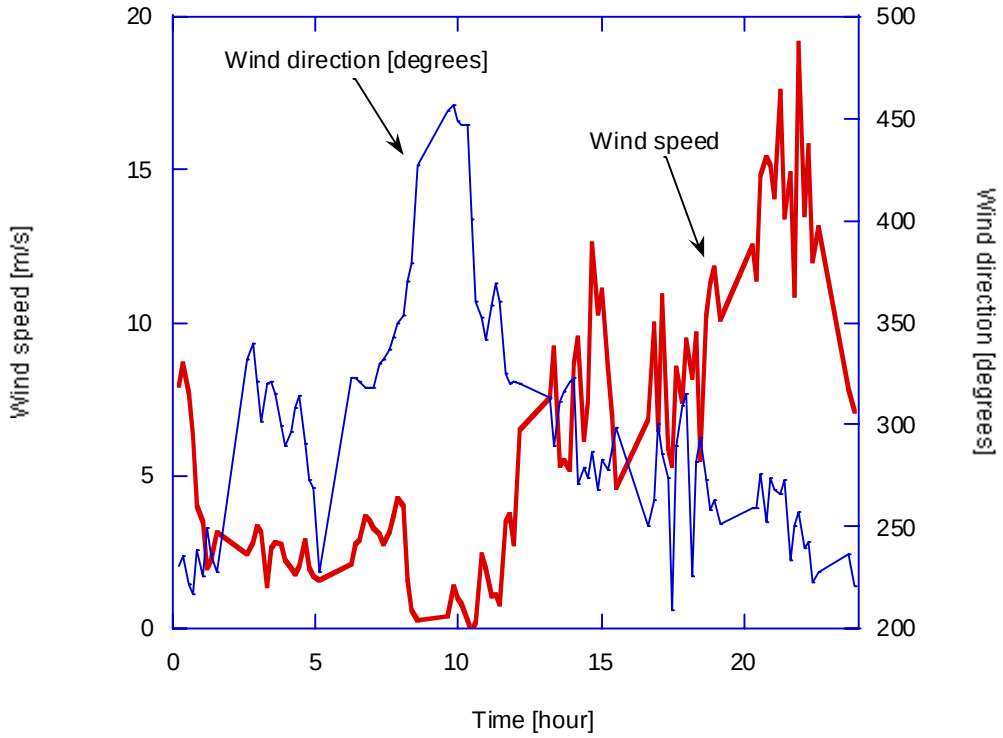

Fig. 5 Ground wind speed (thick line) and direction (thin line) during the day 15/11/99. The wind direction is measured in degrees from the North in the positive sense.

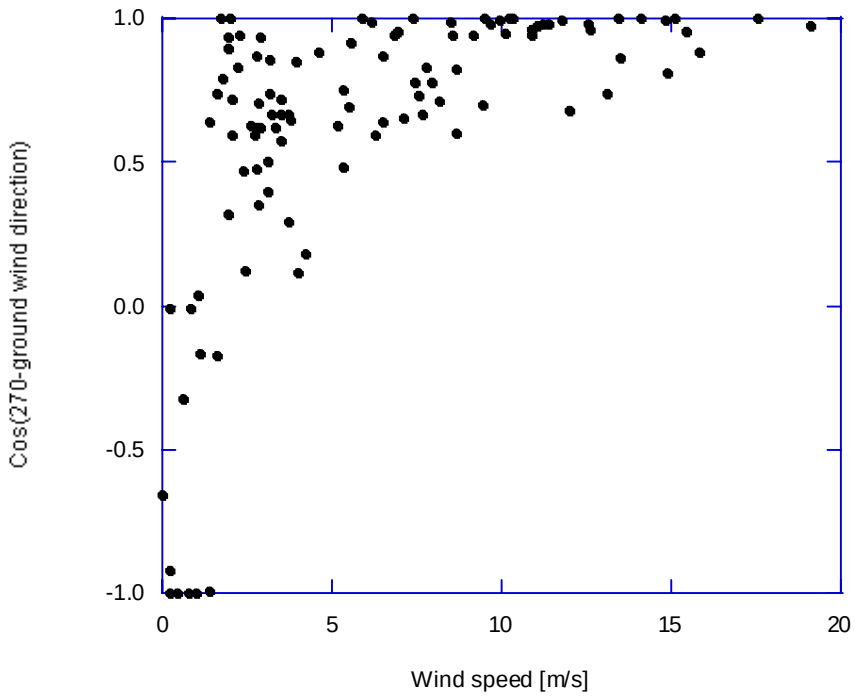

Fig. 6 Wind direction as function of the wind speed. A cosine of 1 indicates wind coming from the West (predominant wind), a –1 cosine indicates wind coming from the East (rare), while a zero cosine indicates wind perpendicular to the E-W baseline.

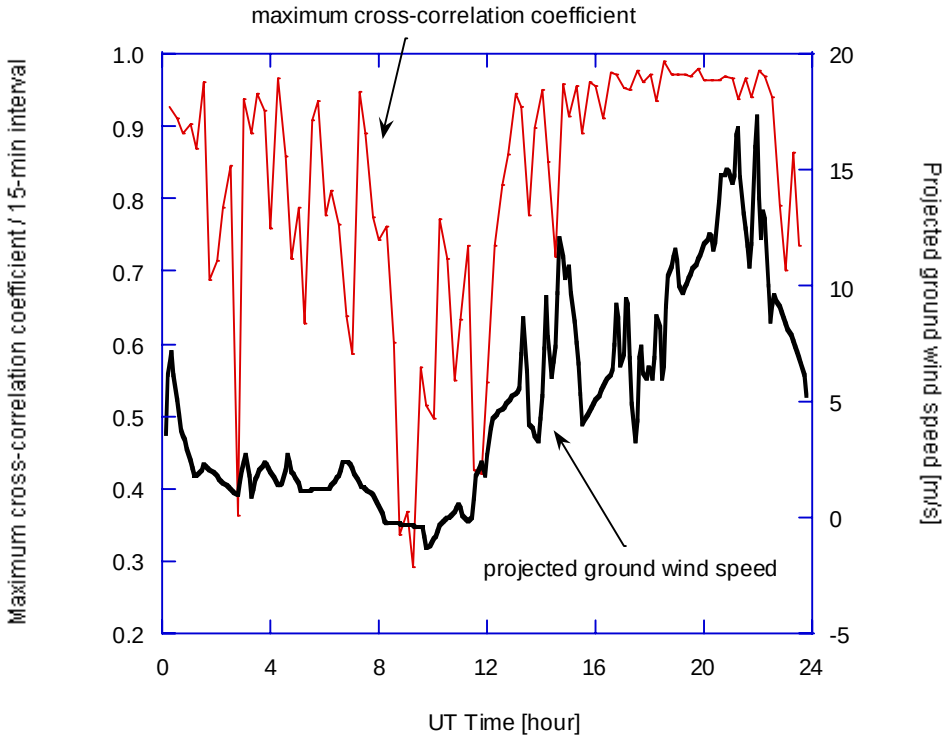

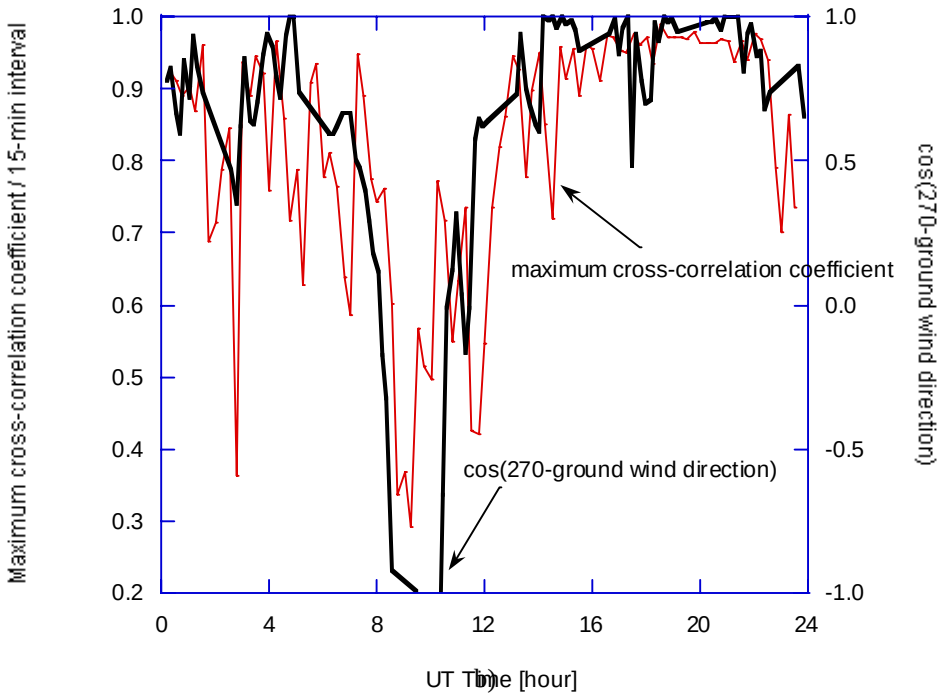

Fig. 7 Comparison between maximum cross-correlation during day 15/11/99, using a 900 sec frame, and a) the projected ground wind speed and b) the ground wind direction.

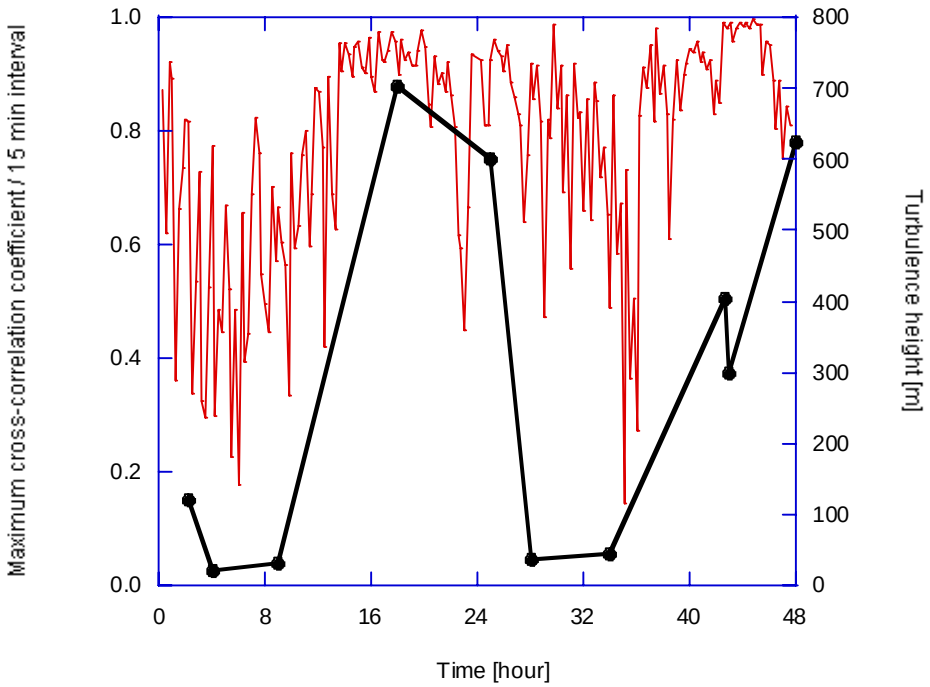

Fig. 8 Result of the cross-correlation for the days 6 and 7 November 1999 (light red line). The solid dots on the black thick line indicate the radiosonde derived heights for the turbulence layer. The time scale is in hours, starting at 0 UT of 6/11/99.

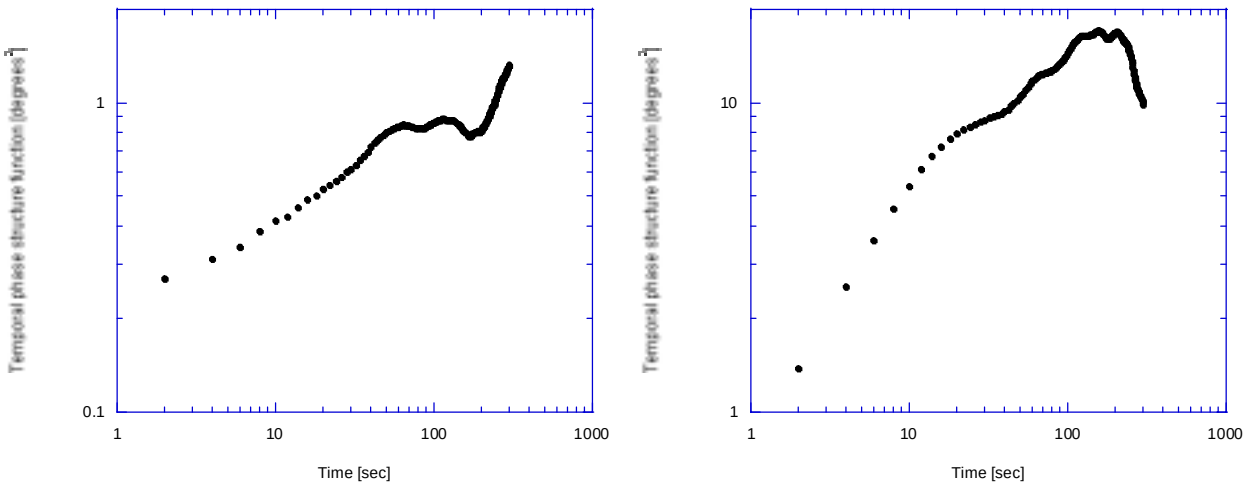

a) b)

Fig. 9 Temporal phase structure function for different times. a) is representative of the low rms phase times (~10 UT) and b) is representative of the large rms phase times (~18 UT) for day 15/11/99.

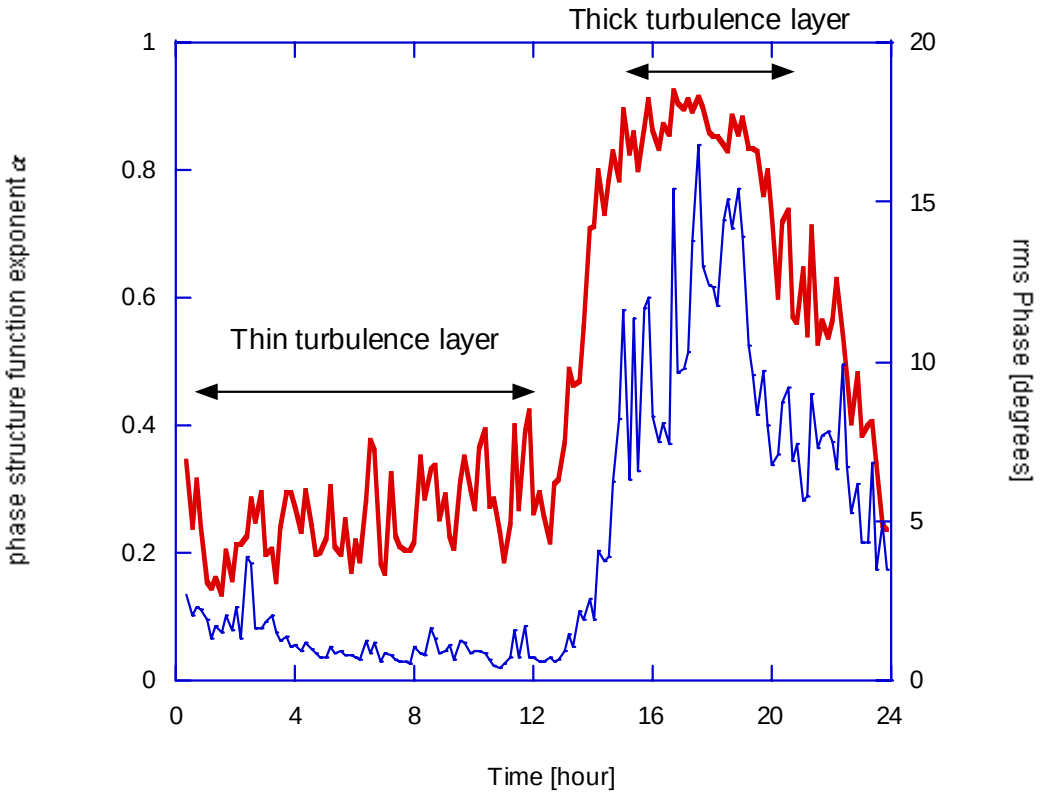

Fig. 10 Daily variation of the α exponent of the temporal phase structure function (thick line) for day 15/11/99 showing the areas with well defined layers and the transition times. The rms phase variation over the same period is also shown (thin line).

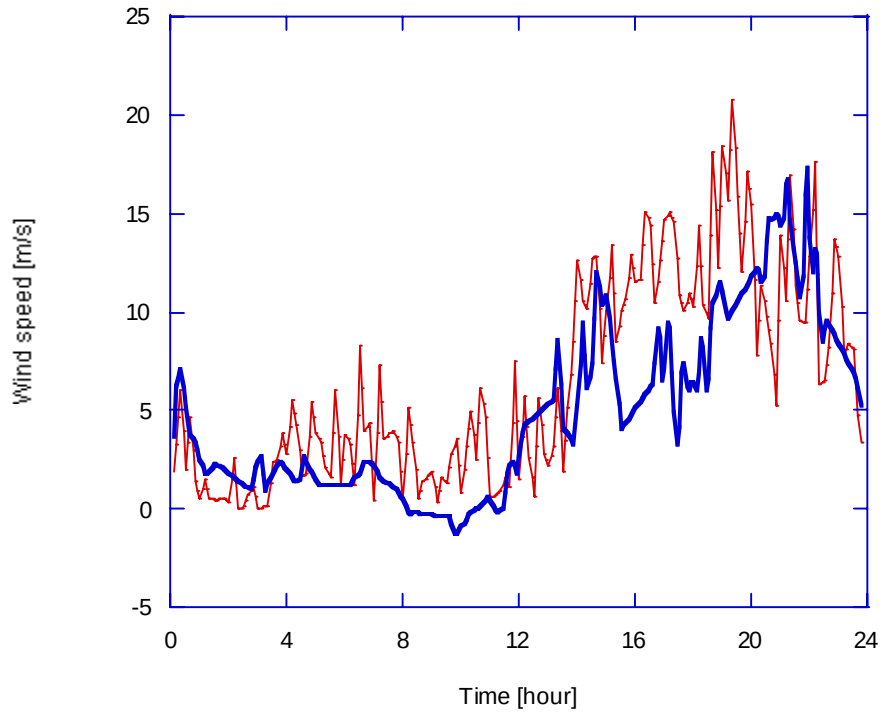

Fig. 11 Ground wind speed projected along the WVRs baseline (thick line) and wind aloft determined from the corner time calculations (thin line) for day 15/11/99.